



ELSEVIER

Contents lists available at SciVerse ScienceDirect

Talanta

journal homepage: www.elsevier.com/locate/talanta

Monitoring the subcellular localization of doxorubicin in CHO-K1 using MEKC – LIF: Liposomal carrier for enhanced drug delivery

Ja-an Annie Ho^{a,b,*}, Nien-chu Fan^b, Amily Fang-ju Jou^a, Li-chen Wu^{c,**}, Tai-ping Sun^d

^a BioAnalytical and Nanobiomedical Laboratory, Department of Biochemical Science and Technology, National Taiwan University, No. 1, Sec. 4, Roosevelt Road, Taipei 10617, Taiwan

^b Department of Chemistry, National Tsing Hua University, No. 101, Sec. 2, Kuang-Fu Road, Hsinchu 30013, Taiwan

^c Department of Applied Chemistry, No. 1 University Road, National Chi Nan University, Puli, Nantou 54561, Taiwan

^d Department of Applied Materials and Optoelectronic Engineering, No. 1 University Road, National Chi Nan University, Puli, Nantou 54561, Taiwan

ARTICLE INFO

Article history:

Received 21 May 2012

Received in revised form

25 June 2012

Accepted 26 June 2012

Available online 16 July 2012

Keywords:

Doxorubicin

Intracellular distribution

Liposome

Micellar electrokinetic chromatography

(MEKC)

Laser-induced fluorescence (LIF)

ABSTRACT

Doxorubicin (DOX) is an extensively used anthracycline that has proven to be effective against a variety of human malignant tumors, such as ovarian or breast cancer. While DOX was administered into cultured cancer cell targets (such as CHO-K1) in either free drug form or in drug carrier-associated form (*i.e.*, DOX encapsulated in the drug delivery carrier), various action of mechanisms for DOX were initiated, among which, it has been long believed that DOX enters the nucleus, interacts with DNA in numerous ways, and finally halts cell proliferation. Aside from its therapeutic effect, regrettably DOX treatment may be accompanied by the occurrence of cardiac and liver toxicity and drug resistance that are attributed from cellular processes involving the parent drug or its metabolites. Liposomal formulation of DOX, known to be capable of attenuating direct uptake of reticuloendothelial system (RES) and prolonging the circulation time in blood, demonstrated reduced toxic side-effects. We herein report the development of a modified MEKC–LIF (Micellar electrokinetic chromatography–Laser-induced fluorescence) method suitable for analyzing DOX in biological samples. The MEKC migration buffer, consisting of 10 mM borate, 100 mM sodium dodecyl sulfate (SDS) (pH 9.3), was found to provide an efficient and stable electrophoretic separation and analysis for DOX. Responses were linear in the range of 11.3–725 ng/mL; the limit of quantitation (LOQ) was found to be 43.1 ng/mL ($S/N=10$) (equivalent to 74.3 nM) and limit of detection (LOD) was calculated as 6.36 ng/mL ($S/N=3$) (equivalent to 11.0 nM). This approach was subsequently employed to compare the intracellular accumulation in three subcellular fractions of DOX-treated CHO-K1 cells. These fractions form a pellet at < 1400g, 1400–14000g, and > 14000g and are enriched in nuclei, organelles (mitochondria and lysosomes), and cytosole components, respectively, resulting from treatment of CHO-K1 cells with 25 μ M (equivalent to 14.5 μ g/mL) of two DOX formats (in free drug form or liposomal form synthesized in current study) for different periods of time. Our results indicated that the most abundant DOX was found in the nuclear-enriched fraction of cells treated for 12 h and 6 h with free and liposomal DOX, respectively, providing direct evidence to confirm the enhanced efficiency of liposomal carriers in delivering DOX into the nucleus. The observations presented herein suggest that subcellular fractionation followed by liquid–liquid extraction and MEKC–LIF could be a powerful diagnostic tool for monitoring intracellular DOX distribution, which is highly relevant to cytotoxicity studies of anthracycline-type anticancer drugs.

© 2012 Elsevier B.V. All rights reserved.

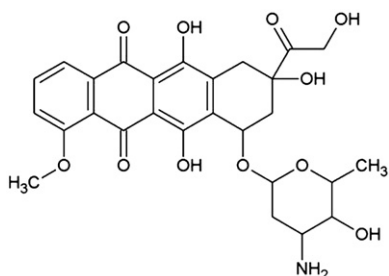
1. Introduction

Anthracyclines are among the most commonly used anticancer drugs, used for more than 30 years and are still considered among

the most useful anticancer agents developed. Doxorubicin (DOX) (structure shown in Scheme 1) is a clinically important anthracycline [1], offering therapeutic effectiveness against a variety of solid tumors, such as leukemia, ovarian cancer, breast cancer, prostate cancer and cervix cancer [2–8]. Despite its extensive clinical utilization, the action mechanisms of anthracycline on cancer cells remain a matter of controversy. The proposed mechanisms are considered as follows [9–11]: (1) inhibition on synthesis of macromolecules due to its intercalation into DNA; (2) DNA damage or lipid peroxidation resulted from the generation

* Corresponding author at: Department of Biochemical Science and Technology, National Taiwan University, No. 1, Sec. 4, Roosevelt Road, Taipei, 10617 Taiwan. Tel.: +886 2 3366 4438; fax: +886 2 3366 2271.

** Corresponding author. Tel.: +886 49 2910960x4890; fax: +886 49 2917956. E-mail addresses: jaho@ntu.edu.tw (J.A. Ho), lw25@ncnu.edu.tw (L.-c. Wu).



Scheme 1. Structure of doxorubicin (DOX).

of free radicals; (3) DNA binding and alkylation; (4) DNA cross-linking; (5) interference with DNA unwinding or DNA strand separation and helicase activity; (6) direct membrane effects; (7) initiation of DNA damage via inhibition of topoisomerase II; and lastly (8) induction of apoptosis in response to topoisomerase II inhibition.

Aside from its therapeutic effect, regrettably DOX treatment also often comes with incidents of cardiac/liver toxicity and drug resistance [2] that may result from cellular processes involving the parent compound or drug metabolites. The oxidative activity of DOX aglycone metabolites, which often leads to the release of mitochondrial Ca^{2+} , the swelling of mitochondria, a change of the mitochondrial membrane potential, and the production of superoxide (O_2^-), may be the factor contributing to acute cardiac and liver toxicity [12]. Needless to say, exploration of possible causes and research into the action mechanism on biological processes (such as drug resistance) and cytotoxicity induced by DOX treatment are considered significant. Moreover, it is also important to study the subcellular localization of DOX, which helps to identify metabolic pathway that DOX takes upon entry of the cell. An efficient and rapid quantification procedure for measurement of DOX or other anthracycline in biological samples is thus in urgent need. Previous studies have reported various analytical approaches for studying DOX, daunorubicin as well as other anthracyclines and their metabolites, including confocal microscopy [13], polarography [14], high-performance liquid chromatography (HPLC) [15–18], displacement chromatography [19], laser flow cytometry [20], and capillary electrophoresis (CE) [1,2,21]. Though chromatographic methods remain the principal analytical approaches for *in vitro* and *in vivo* analysis of anthracyclines due to its superior sensitivity [22,23], the requirement of larger sample size and expensive equipment, complication of sample pretreatment, and consumption of large amounts of solvents have made them less ideal for high-throughput and environmental friendly analytical techniques. CE, on the other hand, is easier to be home-built and capable of analyzing minute quantities of samples. CE related analytical techniques have been widely used as a simple, rapid means to investigate anthracyclines and their metabolites at the single-cell level with no degradation [2,21,24–26].

Drug delivery systems (DDS) are exploited to circumvent some of the non-ideal properties of free drug or conventional formulation and provide better control over the pharmacokinetics (PK) and pharmacodynamics (PD) of the encapsulated drugs relative to free drugs. Liposome has drawn increasing interest from various branches of medicine for its ability to deliver drugs in the optimum dosage range, resulting in improved therapeutic efficacy of the drug and a decline in toxic side effects [27,28], and some examples of success on non-targeted liposomes used in clinical practices have already been demonstrated (*i.e.*, Doxil, which is the trade name for the generic chemotherapy drug—doxorubicin HCl liposome injection; DaunoXome, which is a chemotherapy drug that is given to treat AIDS-related Kaposi's sarcoma). Doctors in

Taiwan prescribe Lipo-dox[®], a pegylated liposomal doxorubicin HCl (TTY Biopharm, Taiwan) for curing ovarian cancer, breast cancer, AIDS-related Kaposi's sarcoma, as this medication is recognized by and can be given full reimbursement by the Taiwan National Health Insurance. It was also found that lower dosage of liposomal DOX was able to efficiently kill more cancer cells *in vitro* and *in vivo* as compared to free DOX [29,30]. However, the quantification of exact amounts of drugs being delivered via liposomal carriers to cells or subcellular fractions, comparing to free drug, has seldom been investigated. In this study, we extend the utilization of a modified MEKC–LIF with reliable separation and good reproducibility to monitor subcellular distribution of DOX, which enters cells via different routes (free form vs. liposomal form). The developed method was used to determine the subcellular accumulation of DOX in cultured Chinese hamster ovary CHO-K1 cells at clinically relevant concentrations, making the method potentially useful for mechanistic studies.

2. Experiment

2.1. Reagent and materials

Doxorubicin hydrochloride (DOX), trypan blue, Nutrient Mixture F-12 Ham (Kaighn's modification) and SDS were purchased from Sigma-Aldrich (St. Louis, MO, USA). Methanol, chloroform and other organic solvents were obtained from Merck KGaA (Darmstadt, Germany). Fetal bovine serum and trypsin–EDTA were acquired from HyClone (Logan, UT, USA). Penicillin and streptomycin were bought from Invitrogen Life Technologies (Carlsbad, CA, USA). Migration solution (BS buffer) used in CE was 10 mM borate buffer containing 100 mM SDS (pH 9.3). Protein assay kit for the quantification of total protein level was purchased from Bio-Rad (Hercules, CA, USA). All buffers were stored at ambient temperature for up to one month, which were prepared using pure Milli-Q water (resistivity < 18 MΩ cm, Millipore, Bedford, MA). Stock solution of DOX (2.9 mg/mL) was made in PBS (phosphate buffered saline, 10 mM), aliquoted in opaque vials, and kept frozen at $-20\text{ }^\circ\text{C}$. To prevent the possible degradation due to the repetitive freeze/thaw cycling of the entire stock solution, an aliquoted vial of DOX stock solution (50 μL) was taken out from freezer and diluted on the day of analysis to prepare fresh working solutions with serial concentrations. SDS used for the migrating solution was prepared by diluting the stock solution (100 mM), which was stable within 1 month. The cell lysis buffer kit (cat. no. 2900) was obtained from Chemicon (Billerica, MA, USA), of which chilled cytoplasmic lysis buffer was premixed with 0.5 mM DTT and 0.1% protease inhibitors prior to be used for lysis of cells.

2.2. Apparatus

Emission spectrum of DOX and DOX encapsulation rate were acquired and determined by a Cary Eclipse spectrofluorometer, which was purchased from Varian (Walnut creek, CA, USA). Particle Analyzer coupled with zeta potential analyzer (Brookhaven Instruments, Holtsville, NY) was utilized for obtaining the size distribution of liposomes and to determine the zeta potential of liposome. A home-built system was used for the MEKC–LIF measurement that consisted of a CZE1000R high-voltage power supply (Spellman, Hauppauge, NY, USA), a ZETALIF EVOLUTION detector (Picometrics Inc., Toulouse, France), in which the 488-nm line of an argon ion laser (Spectra-Physicst, Mountain View, CA) was working as an excitation source, and signal integration/data acquisition system (a personal computer equipped with the HW-2000 chromatography workstation peak ABC system

purchased from JiTeng Trading Pte Ltd., Singapore). Detailed instrumental setup for ZETALIF and a schematic illustration of the CE system are included in supporting information.

2.3. Safety considerations

Extra care should be taken while handling DOX because of the carcinogenic nature of this compound. All samples were sequestered and disposed of according to the MSDS.

2.4. Preparation and characterization of doxorubicin-encapsulated liposomes (liposomal DOX)

Film hydration method was adopted in this study to prepare liposomal DOX [31,32]. In short, the lipid mixture consisting of DPPC, cholesterol, and DPPE (10:10:4 M ratio) was dissolved in a mixture of chloroform, isopropyl ether, and methanol (6:6:1 volume ratio, 4 mL). After sonication of the mixture for 3 min, the organic solvent was evaporated under reduced pressure, leaving a thin lipid film on the round-bottom flask. An aliquot of desired conc. of DOX solution was added to dissolve the lipid film, followed by the sonication for 3 more minutes at 45 °C, producing a light reddish-brown milky suspension. The characterization of liposomal DOX preparation was subjected to dynamic light scattering spectrometric analysis and zeta potential determination. In addition, the optimum DOX/phospholipids ratio and encapsulation rate of DOX were also studied.

2.5. Cell culture and treatment of cells with DOX

Chinese hamster ovary line CHO-K1 cells were obtained from the Culture Collection and Research Center (CCRC) (Hsinchu, Taiwan), and cultured in nutrient mixture F-12 ham (Kaighn's modification) containing 10% fetal bovine serum, 2 mM glutamine, 1% nonessential amino acid, 1 mM pyruvate, 100 units/mL penicillin, and 100 µg/mL streptomycin. About 2×10^6 cells were seeded on 50-mm petri dish and maintained by splitting every 2–3 days through the addition of fresh media in a humidified incubator with 5% CO₂ at 37 °C. After 12 h cell adhesion, cells were treated with optimum conc. of free DOX or liposomal DOX for varied periods of time. The concentration of 25 µM DOX (equivalent to 14.5 µg/mL) was chosen because this was the maximum dosage of DOX that would maintain at least 80% cell viability after co-incubation with cells for 24 h.

After incubation with free DOX or liposomal DOX, respectively, non-adherent cells were removed by washing with PBS. It was followed by the addition of 1 mL of warmed trypsin–EDTA solution to cover the monolayer of cells, allowing the cells to detach from the surface at 37 °C CO₂ incubator within approximately 1 min. Subsequently 9 mL of the cell culture medium were added into the lifted cells to prepare a cell suspension, followed by the centrifugation at 1000g for 5 min. Finally the cell pellet was collected and re-suspended in 1 mL of culture medium solution.

Cell counting was done by mixing 10 µL of well-mixed cell suspension with 10 µL trypan blue stain (0.4%), a few minutes was subsequently given to allow the staining of non-viable cells to proceed for a few minutes. 10 µL of trypan/cell mix was pipetted and dropped at the edge of the cover-slip, allowing the area under the cover-slip to fill by capillary action. Counting of cells was accomplished by visualizing the haemocytometer grid under microscopic observation. Cell viability was calculated as the ratio of no. of viable cell to no. of total cells.

Biologically samples subjected to CE analysis were obtained by collecting the drug-treated cells at 250g for 5 min at 4 °C and washed twice with PBS buffer. The collected cells were incubated

with cell lysis buffer on ice for 15 min, allowing cells to swell. Cell disruption was facilitated by 15 passages through a 27-gauge needle.

The subcellular fractions of cell lysate were obtained similar to that previously reported [2]. The nuclear-enriched fraction was pelleted by centrifugation at 1400g for 10 min at 4 °C, and the supernatant was centrifuged at 14000g for 20 min at 4 °C. The 14000g pellet was designated as the organelle-enriched fraction, while the 14000g supernatant was collected and designated as the cytosole-enriched fraction. The 3 subcellular fractions were then subjected to liquid–liquid extraction as described below.

2.6. Measurement of total protein content

Total cell protein corresponding to the cell count can be used as an index of cell number. In this study, total cell protein was determined using the Bio-Rad protein assay kit based on the method of Bradford, using bovine serum albumin (BSA) as the standard.

2.7. Liquid–liquid extraction (LLE)

The subcellular fractions were subjected to liquid–liquid extraction as described in [2]. The entire sample preparation process took less than 1 h from end of the cell incubation to the introduction of samples into CE system. Addition of 200 µL BS buffer was used to reconstitute the nuclear and organelle fractions. Subsequently the samples were sonicated for 30 min to ensure uniform disruption and optimal release of DOX from the nucleus, cell organelles and other cellular sites. Following the disruption, 600 µL of CHCl₃:MeOH (5:1, v/v) was added to each sample for the extraction of DOX. The samples subjected to extraction underwent two cycles of 5-min vortex mixing to advance the extraction efficiency followed by centrifugation for 10 min at 1000g to separate the chloroform and methanol layers. The less dense aqueous layer and interface emulsification were carefully removed with a syringe and discarded. Finally the desired fraction of sample was collected and dried at 45 °C under a stream of nitrogen. Prior to analysis, 200 µL of PBS buffer was added to the vial for reconstitution, followed by sonication for 15 min.

2.8. MEKC–LIF analysis

MEKC–LIF analyses were carried out on a home-built capillary electrophoretic system with operating temperature at 25 °C. The pretreated samples were separated in an uncoated fused-silica capillary with an internal diameter of 50 µm, outer diameter of 150 µm, effective length of 52 cm, and total length of 65 cm. Migration solution (BS buffer, pH 9.3) used herein consisted of 10 mM borate buffer and 100 mM SDS. The capillary was conditioned by sequential flushing with NaOH (0.1 M), deionized water, and BS buffer for 10 min each. Between runs, the capillary was flushed with BS buffer for 10 min. The samples were injected hydrodynamically into the capillary from the sample vial by gravity-driven siphoning for 5 s (raised 17.5 cm above the outlet vial), thus 2 nL of the sample solution was introduced. A separation voltage (25 kV) was applied using a CZE1000R high-voltage power supply. The fluorescence generated by the excitation of DOX was detected by a Laser Induced Fluorescence Detector. The 488-nm line of an argon ion laser with 25 mW excitation power was employed as excitation source in the LIF detection system. A personal computer equipped with the HW-2000 chromatography workstation peak ABC system was used for signal integration and data acquisition. Calibration curve was obtained by analyzing DOX standards with MEKC–LIF.

3. Results and discussion

3.1. Method development and electropherogram reproducibility

Our MEKC–LIF analysis for DOX was modified based on the design previously described by Anderson et al. [2]. Borate buffer is selected for use herein because phosphate buffer commonly generates a relatively high current resulting in poor separation and resolution. In addition, DOX tends to be neutral or slightly negatively charged in alkaline borate buffer (pH 9.3), which leads to better separation [21].

The effect of SDS concentrations (over the range 10–100 mM) in the BS buffer, which often leads to forming of micelles of different nature and geometry, was examined (data not shown). It was found that increase of the migration time was associated with increasing SDS concentration, suggesting a stronger interaction of DOX with the surfactant micelles at pH 9.3. A 100 mM SDS concentration was adopted as optimal for further experiments as it provided a wide enough window for elution of DOX, well-shaped peaks and reproducible migration time.

As mentioned previously, reproducibility of migration time is essential for identification and quantification of DOX. Drifting in migration time might cause errors in peak identification. Fig. 1 shows the representative electropherograms for DOX, and the precision in migration time was high at all runs for intraday runs ($\leq 1.1\%$ RSD), and for interday runs ($\leq 3.6\%$ RSD). Table 1 revealed that the precision in fluorescence signal was acceptable at all concentrations for intraday runs ($\leq 2.1\%$ RSD) and for interday runs ($\leq 3.8\%$ RSD).

3.2. Cytotoxic and therapeutic effects and cellular uptake of free-DOX and liposomal DOX on CHO-K1 cells

Liposomal formulations of the chemotherapeutics (i.e., Doxil[®], ALZA Corp.) showed better efficiency in eliminating the cardiotoxic effect, enhancing antitumor activity, and advancing therapeutic index [33–36]. To evaluate the cytotoxic effect of liposomal DOX and free-DOX on killing of CHO-K1 cells, the viability of cells were investigated by trypan blue assay. Fig. 2A

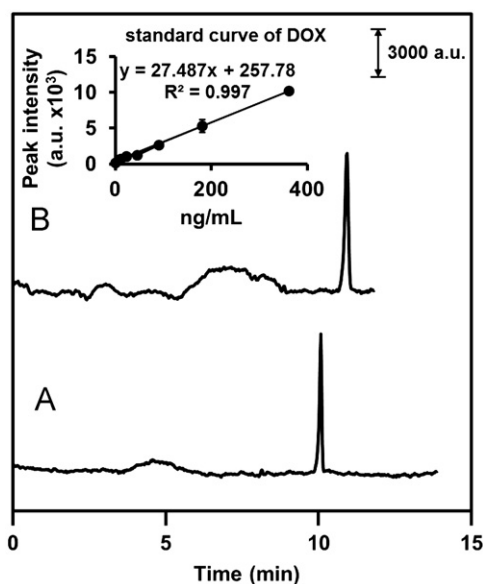


Fig. 1. Electropherograms for (A) the standard solution of DOX, 300 ng/mL (equivalent to 517 nM), prepared in phosphate buffered saline (pH=7.4); (B) CHO-K1 cell lysate spiked with 300 ng/mL (equivalent to 517 nM) of DOX. Inset shows the standard curve for DOX. Migration buffer: 10 mM borate buffer containing 100 mM sodium dodecyl sulfate (pH 9.3), separation voltage, 25 kV.

Table 1

Analytical performance of the LLE method in conjunction with modified MEKC–LIF detection.

DOX (ng/mL)	Recovery (% ± SD)	Precision (%RSD)		LOD (ng/mL)
		Intraday	Interday	
181	98.2 ± 3.7	2.04	3.73	6.36
527	97.2 ± 1.6	0.98	1.60	
n=3				

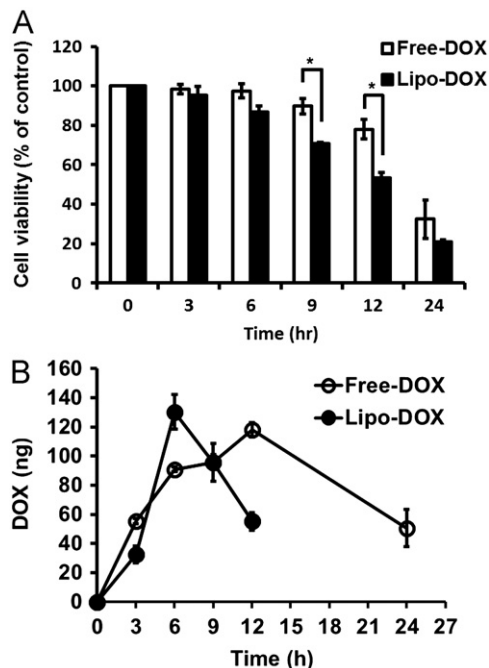


Fig. 2. (A) Cytotoxicity of free DOX and liposomal DOX toward CHO-K1 cells (white bar, free DOX; black bar, liposomal DOX) (* $p < 0.05$). (B) Effect of the DOX formulation (free vs. liposomal) on cellular uptake in CHO-K1 cells (hollow circle, free DOX; solid circle, liposomal DOX).

indicates the viability of CHO-K1 cell with 25 μ M free DOX or liposomal DOX. 95% and 85% of CHO-K1 cells remain viable after 6 h incubation with free-DOX or liposomal DOX, respectively, revealing the combination of such dose and treatment time exhibited low cytotoxicity toward CHO-K1 cells. Furthermore it was found that the cell viability decreased with time length of treatment for both free DOX group and liposomal DOX group. Liposomal formulation showed better therapeutic result than that of free DOX in eliminating CHO-K1 cells (70% vs. 90% at 9 h; 55% vs. 80% at 12 h). The results clearly suggested the remarkable capability of liposomal DOX to deliver its cargo, DOX, into cells, which significantly increased the efficacy of therapy (* $p < 0.05$).

Fig. 2B shows the time-dependent cellular uptake/drug accumulation in CHO-K1 cells with exposure to same concentration of free DOX and liposomal DOX. It was observed that the accumulation of DOX in CHO-K1 treated with free DOX reached maximum level at 12 h, whereas in liposomal DOX-treated cells, the maximum level time was achieved much earlier (at 6 h). The results suggest that the cancer cell elimination capability of DOX-encapsulated liposomes was most likely attributable to the fact that liposomal carrier enhances the efficiency in delivering its cargo to diseased cells as compared with free DOX. Furthermore it was also noted that the amount of cellular accumulated DOX dropped off for both groups (free vs. liposomal DOX), presumably it was because the significant cytotoxic effect of free DOX and liposomal

DOX (as indicated in Fig. 2A) exerted on the CHO-K1 after 6 h and 12 h, respectively.

3.3. Characterization of liposomal DOX

The characteristics of liposome formulation, including particle size, surface charge property, and drug/lipid ratio possess an influential effect on the cellular uptake [37–39]. As reported by Storm et al. [40], the size of the colloidal carriers and their surface characteristics are critical to the biological fate of nanoparticles. A smaller size and a hydrophilic surface are essential in achieving the reduction of opsonization reactions and subsequent clearance by macrophages. In addition, the size and surface properties of the drug carriers also have an effect on the adsorptive endocytosis. If the surface charge of the nanoparticles is negatively charged and hydrophilic, it shows greater affinity to adsorptive enterocytes and M-cells of Peyer's patches in the GI tract, suggesting that a combination of size, surface charge and hydrophilicity play a major role in affinity [41]. The zeta potential of nanoparticles is used to characterize the surface charge property of nanoparticles or to determine whether a charged active material is encapsulated within the center of the nanocarrier or adsorbed onto the surface. The value of zeta potential reflects the electrical potential of particles and is influenced by the composition of the particle and the medium where they are dispersed [42].

In this study, the particle size and the zeta potential of the Dox-encapsulated liposomes (liposomal DOX) were examined at different lipid (μmole):DOX (μg) ratios (by fixing the DOX amount and altering the amount of lipid used). The particle size and the zeta potential of liposomal DOX prepared by film hydration method were in the range of 740–1300 nm, and -0.56 – 1.21 mV, respectively. The particle size of the liposomal DOX increased in parallel with lipid:DOX ratio whereas the zeta potential of the liposomal DOX was found to be independent of the lipid:DOX ratio (shown in Table 2).

3.4. Subcellular localization of free DOX and liposomal DOX

Previous studies have demonstrated that the intracellular accumulation and the subcellular localization of anti-cancer agents might exert a significant effect on their cytotoxic potency and subsequently contribute to their pharmacological features [13,43–45]. In this study, MEKC–LIF analysis was employed to monitor the cellular uptake and subcellular distribution of DOX, either in free or liposomal form, after co-incubation with CHO-K1 cells for 6 h. To investigate the efficiency of DOX being delivered to the CHO-K1 cells via liposomes, 6 h DOX treatment, liquid–liquid extraction of DOX from cell lysates, followed by the MEKC–LIF analysis were carried out. Fig. 3A illustrates the DOX accumulation in CHO-K1 cells treated with different formulated liposomal DOX for 6 h (lipid:DOX ratio varies from 0.33 to 1.1). Our results suggested that liposomal DOX with lipid:DOX ratio of 1.1 showed the finest cellular uptake or cellular accumulation among experimental groups. We believed that such phenomenon was due to the

hydrophilicity and slightly negative charge of the liposomal outer surface, and more DOX molecules were contained inside of a liposome. The MEKC–LIF analysis described above was employed to estimate the amounts of DOX in different subcellular fractions by differential centrifugation (as indicated in Scheme 1B). As described by Anderson et al., such strategy has been proven useful in determining differences in subcellular distribution of DOX [2]. The composition of subcellular fractions has been extensively studied previously [46–48]. According to those previous reports, the fraction pelleted at 1400g contains nearly all of the nuclei [46] and a small fraction of unbroken and partially broken cells, mitochondria, and large sheets of plasma membrane [46–48]. The fraction pelleted at 14000g contains mostly mitochondria and lysosomes and also large microsomes [48]. The supernatant remaining after pelleting at 14000g is considered the cytosole-enriched fraction because soluble components, small membrane bound structures, and microsomes

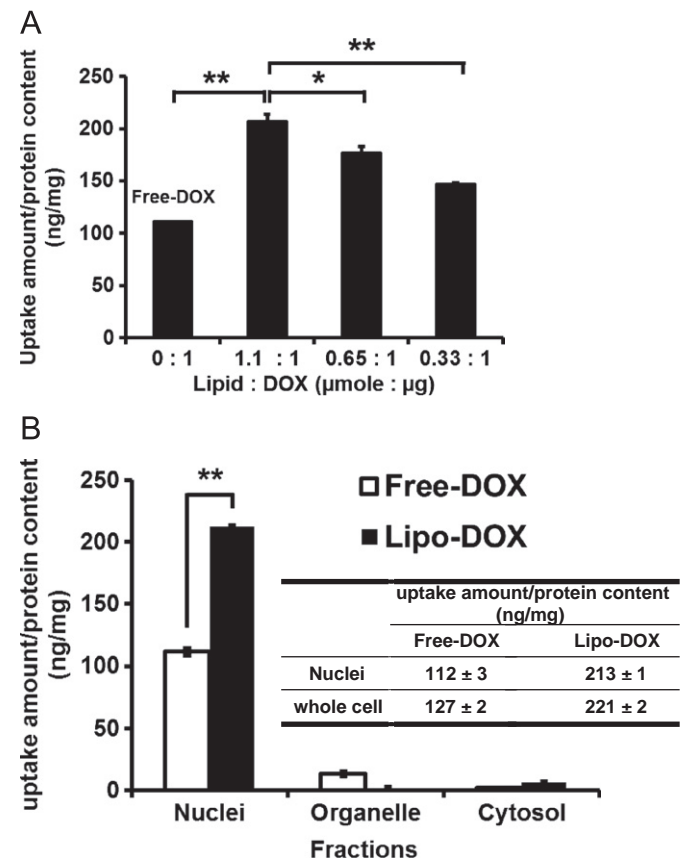


Fig. 3. (A) Drug accumulation in CHO-K1 cells exposed to three liposomal DOXs with different lipid:DOX ratio (the phospholipid:DOX ratios of the liposomal DOX preparations used herein were 1.1 $\mu\text{mol}/\mu\text{g}$, 0.65 $\mu\text{mol}/\mu\text{g}$ and 0.33 $\mu\text{mol}/\mu\text{g}$, respectively) (* $p < 0.05$, ** $p < 0.01$); (B) intracellular distribution of DOX in CHO-K1 cells treated with free DOX and liposomal DOX (white bar, free DOX; black bar, liposomal DOX) (** $p < 0.01$).

Table 2

The characteristics of various liposomal DOX synthesized in this study.

Lipid(μmole):DOX(μg)	1.1:1	0.65:1	0.33:1	Free-DOX
Mean diameter (nm)	1.3×10^3	1.1×10^3	7.4×10^2	
Volume of liposome (mL)	9.9×10^{-13}	6.8×10^{-13}	2.1×10^{-13}	
DOX concentration ($\mu\text{g}/\text{mL}$)	14.5	14.5	14.5	14.5
(equivalent to, μM)	25.0	25.0	25.0	25.0
DOX concentration after lysis ($\mu\text{g}/\text{mL}$)	1.4	1.0	1.5	
DOX molecules per liposome	1.5×10^4	1.0×10^4	3.1×10^3	–
Zeta potential (mV)	-0.56	-0.68	1.21	

were found in the cytoplasm [48]. Fig. 3B shows the subcellular localization of DOX in either free or liposomal form. It was found that most of the DOX were accumulated in the nuclei fraction of CHO-K1 for both DOX forms after 6 h treatment; moreover, almost 2-fold more DOX, delivered by liposomal carrier, were accumulated in nuclei than the traditional free DOX. Our results suggest that the better therapeutic action of liposomal DOX was achieved by the efficient delivery of anthracycline into the nucleus leading to its interaction with DNA.

4. Conclusions

Liposomes, as drug carriers for anthracycline, *i.e.* DOX, have been long believed to be a possible solution for such a dilemma in cancer therapy, leading to better therapeutic outcome. In the present study, the use of differential centrifugation, liquid–liquid extraction (LLE) and a modified MEKC–LIF method provided clear evidence that the improved therapeutic effect of liposomal DOX was due to the efficient delivery of DOX into the nucleus of cancerous cells. The combination of LLE and modified MEKC–LIF method enables the quantification of anthracycline level accumulated in nucleus (intercalated in DNA) or incorporated in other intracellular fractions. Such an analytical strategy has been demonstrated herein to be useful in studying the mechanisms of action for anthracycline delivered by liposomal carriers.

Acknowledgments

Authors are thankful to the National Science Council in Taiwan, under grants 92-2120-M-260-001, 98-2113-M-007-013-MY3, 99-2113-M-260-002-MY2 and 100-2113-M-002-016-MY2.

Appendix A. Supporting information

Supplementary data associated with this article can be found in the online version at <http://dx.doi.org/10.1016/j.talanta.2012.06.077>.

References

- [1] Y. Chen, R.J. Walsh, E.A. Arriaga, *Anal. Chem.* 77 (2005) 2281–2287.
- [2] A.B. Anderson, C.M. Ciriacks, K.M. Fuller, E.A. Arriaga, *Anal. Chem.* 75 (2003) 8–15.
- [3] N. Katsumata, Y. Fujiwara, T. Kamura, T. Nakanishi, M. Hatae, D. Aoki, K. Tanaka, H. Tsuda, S. Kamiura, K. Takehara, T. Sugiyama, J. Kigawa, K. Fujiwara, K. Ochiai, R. Ishida, M. Inagaki, K. Noda, *Jpn. J. Clin. Oncol.* 38 (2008) 777–785.
- [4] G.G. Kimmick, C. Cirrincione, D.B. Duggan, K. Bhalla, N. Robert, D. Berry, L. Norton, S. Lemke, I.C. Henderson, C. Hudis, E. Winer, *Breast Cancer Res. Treat.* 113 (2009) 479–490.
- [5] F.S. Shaheen, P. Znojek, A. Fisher, M. Webster, R. Plummer, L. Gaughan, G.C. Smith, H.Y. Leung, N.J. Curtin, C.N. Robson, *PLoS One* 6 (2011) e20311.
- [6] A. Goel, B.B. Aggarwal, *Nutr. Cancer* 62 (2010) 919–930.
- [7] Y. Terai, M. Kanemura, H. Sasaki, S. Tsunetoh, Y. Tanaka, Y. Yamashita, K. Yamamoto, I. Narabayashi, M. Ohmichi, *Int. J. Clin. Oncol.* 14 (2009) 56–62.
- [8] K. Effenberger-Neidnicht, R. Schobert, *Cancer Chemother. Pharmacol.* 67 (2011) 867–874.
- [9] A. Bodley, L.F. Liu, M. Israel, R. Seshadri, Y. Koseki, F.C. Giuliani, S. Kirschenbaum, R. Silber, M. Potmesil, *Cancer Res.* 49 (1989) 5969–5978.
- [10] G. Minotti, P. Menna, E. Salvatorelli, G. Cairo, L. Gianni, *Pharmacol. Rev.* 56 (2004) 185–229.
- [11] D.A. Gewirtz, *Biochem. Pharmacol.* 57 (1999) 727–741.
- [12] S. Licata, A. Saponiero, A. Mordente, G. Minotti, *Chem. Res. Toxicol.* 13 (2000) 414–420.
- [13] U. Beyer, B. Rothen-Rutishauser, C. Unger, H. Wunderli-Allenspach, F. Kratz, *Pharm. Res.* 18 (2001) 29–38.
- [14] S.M. Golabi, D. Nematollahi, *J. Pharm. Biomed. Anal.* 10 (1992) 1053–1057.
- [15] I. Tamaro, A. Genazzani, P. Canonico, G. Grosa, *Eur. J. Drug Metab. Pharmacokinet.* 34 (2009) 19–26.
- [16] Y. Qi, J. Huang, *J. Chromatogr. A* 959 (2002) 85–93.
- [17] G. Wei, S. Xiao, D. Si, C. Liu, *Biomed. Chromatogr.* 22 (2008) 1252–1258.
- [18] C.A. Farthing, D.E. Farthing, S. Koka, T. Larus, I. Fakhry, L. Xi, R.C. Kukreja, D. Sica, T.W. Gehr, *J. Chromatogr. B. Anal. Technol. Biomed. Life Sci.* 878 (2010) 2891–2895.
- [19] C.S. Sastry, J.S. Lingewara Rao, *Talanta* 43 (1996) 1827–1835.
- [20] A. Krishan, A. Sauerteig, K. Gordon, C. Swinkin, *Cancer Res.* 46 (1986) 1768–1773.
- [21] J. Mbuna, T. Kaneta, T. Imasaka, *Electrophoresis* 31 (2010) 1396–1404.
- [22] J. van Asperen, O. van Tellingen, J.H. Beijnen, *J. Chromatogr. B Biomed. Sci. Appl.* 712 (1998) 129–143.
- [23] P. Zhao, A.K. Dash, *J. Pharm. Biomed. Anal.* 20 (1999) 543–548.
- [24] A.B. Anderson, J. Gergen, E.A. Arriaga, *J. Chromatogr. B Anal. Technol. Biomed. Life Sci.* 769 (2002) 97–106.
- [25] S.N. Krylov, D.A. Starke, E.A. Arriaga, Z. Zhang, N.W. Chan, M.M. Palcic, N.J. Dovichi, *Anal. Chem.* 72 (2000) 872–877.
- [26] S.N. Krylov, E. Arriaga, Z. Zhang, N.W. Chan, M.M. Palcic, N.J. Dovichi, *J. Chromatogr. B Biomed. Sci. Appl.* 741 (2000) 31–35.
- [27] Y. Kaneda, *Adv. Drug Delivery Rev.* 43 (2000) 197–205.
- [28] B.S. Ding, T. Dziubla, V.V. Shuvaev, S. Muro, V.R. Muzykantov, *Mol. Interv.* 6 (2006) 98–112.
- [29] R.E. Eliaz, F.C. Szoka Jr., *Cancer Res.* 61 (2001) 2592–2601.
- [30] L.D. Mayer, M.B. Bally, P.R. Cullis, S.L. Wilson, J.T. Emerman, *Cancer Lett.* 53 (1990) 183–190.
- [31] J.A. Ho, M.R. Huang, *Anal. Chem.* 77 (2005) 3431–3436.
- [32] J.A. Ho, L.C. Wu, M.R. Huang, Y.J. Lin, A.J. Baeumner, R.A. Durst, *Anal. Chem.* 79 (2007) 246–250.
- [33] A. Gabizon, D. Goren, R. Cohen, Y. Barenholz, *J. Controlled Release* 53 (1998) 275–279.
- [34] P. Carter, *Nat. Rev. Cancer* 1 (2001) 118–129.
- [35] J. Liu, H. Lee, M. Huesca, A. Young, C. Allen, *Cancer Chemother. Pharmacol.* 58 (2006) 306–318.
- [36] T.A. Elbayoumi, V.P. Torchilin, *Eur. J. Pharm. Sci.* 32 (2007) 159–168.
- [37] J. Wu, A. Lee, Y.H. Lu, R.J. Lee, *Int. J. Pharm.* 337 (2007) 329–335.
- [38] R.B. Campbell, S.V. Balasubramanian, R.M. Straubinger, *Biochim. Biophys. Acta* 1512 (2001) 27–39.
- [39] M.P. Desai, V. Labhasetwar, E. Walter, R.J. Levy, G.L. Amidon, *Pharm. Res.* 14 (1997) 1568–1573.
- [40] G. Storm, S.O. Belliot, T. Daemen, D.D. Lasic, *Adv. Drug Delivery Rev.* 17 (1995) 31–48.
- [41] P. Jani, G.W. Halbert, J. Langridge, A.T. Florence, *J. Pharm. Pharmacol.* 41 (1989) 809–812.
- [42] P. Couvreur, G. Barratt, E. Fattal, P. Legrand, C. Vauthier, *Crit. Rev. Ther. Drug Carrier Syst.* 19 (2002) 99–134.
- [43] D. Goren, A.T. Horowitz, D. Tzemach, M. Tarshish, S. Zalipsky, A. Gabizon, *Clin. Cancer Res.* 6 (2000) 1949–1957.
- [44] J. Wu, Y. Lu, A. Lee, X. Pan, X. Yang, X. Zhao, R.J. Lee, *J. Pharm. Pharm. Sci.* 10 (2007) 350–357.
- [45] D.H. Xu, J.Q. Gao, W.Q. Liang, *Pharmazie* 63 (2008) 646–649.
- [46] J. Meijer, A. Bergstrand, J.W. Depierre, *Biochem. Pharmacol.* 36 (1987) 1139–1151.
- [47] E.A. Madden, B. Storrie, *Anal. Biochem.* 163 (1987) 350–357.
- [48] J.M. Graham, D. Rickwood, IRL Press at Oxford University Press, Oxford; New York, 1997.